

Angle-resolved photoemission spectra of the Hubbard model

Th. A. Maier,¹ Th. Pruschke,² and M. Jarrell¹¹*Department of Physics, University of Cincinnati, Cincinnati, Ohio 45221*²*Center for Electronic Correlations and Magnetism, Theoretical Physics III, Institute for Physics, University of Augsburg, 86135 Augsburg, Germany*

(Received 14 November 2001; revised manuscript received 28 March 2002; published 1 August 2002)

We discuss spectra calculated for the two-dimensional Hubbard model in the intermediate coupling regime with the dynamical cluster approximation, which is a nonperturbative approach. We find a crossover from a normal Fermi liquid with a Fermi surface closed around the Brillouin-zone center at large doping to a non-Fermi liquid for small doping where the Fermi surface is holelike, closed around $M = (\pi, \pi)$. The topology of the Fermi surface at low doping indicates a violation of Luttinger's theorem. We discuss different ways of presenting the spectral data to extract information about the Fermi surface. A comparison to recent experiments is presented.

DOI: 10.1103/PhysRevB.66.075102

PACS number(s): 71.27.+a, 71.18.+y, 71.10.-w

I. INTRODUCTION

The rich phenomenology of high- T_c superconductors¹ has stimulated strong experimental and theoretical interest in the field of strongly correlated electron systems. Apart from the anomalously high transition temperatures, these compounds are also of interest due to their unusual normal-state properties. Most of these anomalous properties are found in spectra and transport quantities, i.e., they are intimately linked to the dynamics of the electronic degrees of freedom. Thus, much of the experimental and theoretical effort has concentrated on the development of an understanding of the single-particle dynamics. Among the fundamental and controversial questions are whether the cuprates can be described as a Fermi liquid and what shape and volume a possible Fermi surface will have.

In this connection, one of the most informative experimental probes of the cuprates is angle-resolved photoemission spectroscopy (ARPES). The development in this field, again largely stimulated by the interest in the physics of high- T_c superconductors, has led to a tremendous increase in angle and energy resolution.^{2,3} ARPES is now able to access the low-energy behavior of single-particle spectra, especially the shape and topology of the cuprate Fermi surface. This has led to the discovery of shadow bands^{1,4} and pseudogap formation in the underdoped cuprates.¹ Recently, the single-particle self-energy was extracted from the ARPES data, showing extremely interesting behavior especially close to $(\pi/2, \pi/2)$ on the Fermi surface.⁵

A large number of the more recent ARPES experiments has concentrated on Fermi-surface mapping. Some of these experiments seem to indicate that, at least for $\text{La}_{2-x}\text{Sr}_x\text{CuO}_4$ (LSCO), the Fermi surface switches from being holelike, centered at $M = (\pi, \pi)$ for low doping, to being electronlike, centered at the zone center $\Gamma = (0, 0)$ for high doping with a volume consistent with the doping level.^{3,6,7} In other results, particularly for bilayer compounds like $\text{YBa}_2\text{Cu}_3\text{O}_{6+\delta}$ (YBCO) or $\text{Bi}_2\text{Sr}_2\text{CaCu}_2\text{O}_{8+\delta}$ (Bi2212),^{3,8} the Fermi surface seems to remain holelike independent of the doping level. Especially for those latter compounds, further complications in the experiments arise from superstructures due to umklapp

scattering and the possibility of bilayer splittings in YBCO and Bi2212.^{3,9} In the single-layer compound $\text{Bi}_2\text{Sr}_2\text{CuO}_{6+\delta}$ (Bi2201), however, where the complication of bilayer splitting is not present, a Fermi surface that remains holelike over the whole doping regime has also been observed recently.¹⁰

Furthermore, in the underdoped regime one can observe additional changes in the Fermi-surface topology that frequently develop in connection with the possibility of stripe formation in LSCO.³

The presence of a large Fermi surface has been taken as a validation of Luttinger's theorem; however, other results find that the Fermi-surface volume, at least in the underdoped regime, is too small,⁸ which would point towards a violation of Luttinger's theorem. Furthermore, recent experiments seem to indicate that the Fermi surface near $X = (\pi, 0)$ actually bifurcates into two parts.¹¹ This splitting has been interpreted in terms of strong interlayer coupling,⁹ but could equally well result from shadow Fermi-surface formation due to coupling of the electrons to strong antiferromagnetic fluctuations around the X points.⁸ Recent experiments^{12,13} on the bilayer compound Bi2212 and single-layer material Bi2201, however, show evidence that the observed doubling of the Fermi surface originates in the bilayer splitting effect. Nevertheless, a consistent experimental picture concerning both shape and volume of the Fermi surface is at present not available and a theoretical investigation of the generic features to be expected based on a model calculation is necessary.

Early in the theoretical investigation of the high- T_c cuprates it was realized that the two-dimensional (2D) Hubbard model

$$H = \sum_{i,j,\sigma} t_{ij} c_{i\sigma}^\dagger c_{j\sigma} + \frac{U}{2} \sum_{i\sigma} c_{i\sigma}^\dagger c_{i\sigma} c_{i\bar{\sigma}}^\dagger c_{i\bar{\sigma}} \quad (1)$$

in the intermediate coupling regime, or closely related models such as the t - J model, probably capture the essential physics.¹⁴ In the wake of this conjecture, a huge effort has been directed to the study of these models.¹⁵ There is now a general consensus that the appropriate parameter regime for the cuprates is the intermediate coupling regime where the Coulomb parameter U is roughly equal to the bandwidth.

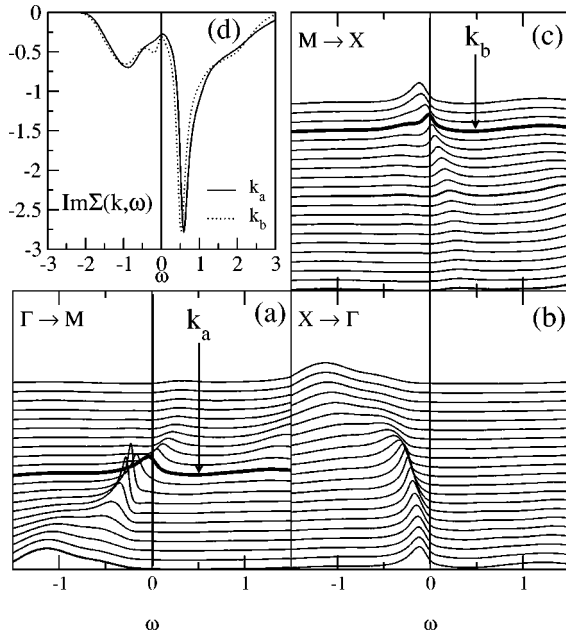


FIG. 2. (a)–(c) The single-particle spectrum $A(\mathbf{k}, \omega)$ for $U = 2$ eV, $T = \frac{1}{30}$ eV, $\delta = 0.05$, and $N_c = 16$ along certain high-symmetry directions (spectra for different \mathbf{k} are shifted along the y axis). The thick lines in (a) and (c) indicate the spectra which cross the Fermi energy with a peak closest to $\omega = 0$. In (b), no such peak which crosses the Fermi energy is found. (d) The imaginary part of the self-energy versus frequency at the Fermi-surface crossing found in (a) and (c).

the maximum entropy method.³⁰ Finally, the self-energy is interpolated onto the full Brillouin zone using Akima splines, which is a sensible step as long as the assumption of a slow variation in \mathbf{k} space is valid. Note that it is very important to interpolate irreducible quantities like the self-energy and *not*, for example, the cluster Green function itself.

III. RESULTS

For a proper description of the CuO_2 planes of the high- T_c cuprates within the Hubbard model (1) it is generally accepted that the tight-binding dispersion has the form

$$t_{\vec{k}} = -2t[\cos(k_x) + \cos(k_y)] - 4t'\cos(k_x)\cos(k_y) \quad (2)$$

with a nearest-neighbor hopping amplitude $t > 0$ and a next-nearest neighbor hopping amplitude t' , which, in principle, can have any sign. From band structure calculations and the general form of the measured Fermi surface, especially in the overdoped regime, conventionally a negative t' is inferred.³¹ Such a negative t' would naturally lead to a Fermi surface closed around the Brillouin-zone corner M . The interesting question, however, is whether the Fermi surface closed around the M point observed experimentally in the low-doping region is a mere band-structure effect or induced by correlations. Weak-coupling treatments of the 2D Hubbard model indicate that such a change of the shape, but not the volume, of the Fermi surface due to the interactions is indeed possible.^{17,32} On the other hand, results from early finite size approximations suggest that both the shape and the volume

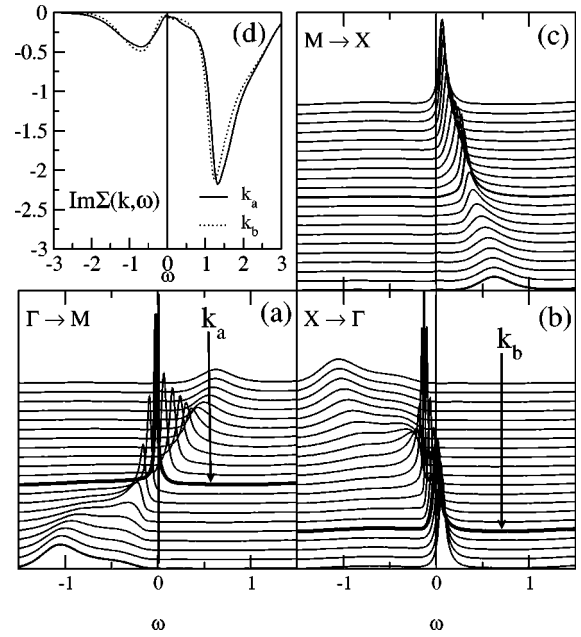


FIG. 3. (a)–(c) The single-particle spectrum $A(\mathbf{k}, \omega)$ $\delta = 0.20$ along certain high-symmetry directions. Other parameters are as in Fig. 2. The thick lines in (a) and (b) indicate the spectra which cross the Fermi energy with a peak closest to $\omega = 0$. In (c), no such peak which crosses the Fermi energy is found. (d) The imaginary part of the self-energy versus frequency at the Fermi-surface crossing found in (a) and (b).

of the Fermi surface will change.³³ Thus, to obtain insight into the effects of correlations on the structure of the Fermi surface and distinguish them from pure band-structure effects, we concentrate on the case $t' = 0$ in this paper.

In the following we set $t = 1/4$ eV in accordance with typical values extracted from the experiments and the band structure and choose $U = W = 2$ eV. This value of U is sufficiently large enough that for $N_c \geq 4$ a Mott gap is present in the half filled model.³⁴ We performed our simulations over a range of temperatures, but will present results for $T = 0.033$ eV only, which is roughly room temperature. A pseudogap due to short-range spin correlations is also present in the weakly doped model for slightly lower temperatures.²²

The single-particle spectra for certain high symmetry directions are plotted in Figs. 2 and 3 for $n = 0.95$ and $n = 0.80$, respectively. We use the standard convention to identify the high symmetry points in the zone $\Gamma = (0,0)$, $M = (\pi, \pi)$, and $X = (\pi, 0)$. For $n = 0.95$ the peak in the spectrum crosses the Fermi energy along the $\Gamma \rightarrow M$ and $M \rightarrow X$ directions, while for $n = 0.80$ the second crossing appears along $X \rightarrow \Gamma$. The imaginary part of the self energy at these crossing points is plotted versus frequency in Figs. 2(d) and 3(d).

One very interesting feature of the spectra at low doping, Fig. 2, is that the peak near $(\pi/2, \pi/2)$ broadens dramatically before crossing the Fermi energy. Near X , on the other hand, one does not observe any dramatic change in the spectrum when crossing the Fermi energy. This indicates that near $(\pi/2, \pi/2)$ holelike quasiparticle excitations with $k < k_F$ ap-

pear to have longer lifetimes than electronic excitations with $k > k_F$. This asymmetry between particles and holes near the Fermi surface is a strong indication of non-Fermi-liquid (NFL) behavior, at least along the $\Gamma \rightarrow M$ direction.

It is also quite instructive to look at the imaginary part of the self-energy at the \mathbf{k} points where the peak in the spectrum crosses the Fermi energy [Fig. 2(d)]. In particular at the crossing point \mathbf{k}_b close to $(\pi, 0)$, $\text{Im} \Sigma(\mathbf{k}_b, \omega)$ shows a striking asymmetry in the low-frequency regime as compared to $\text{Im} \Sigma(\mathbf{k}_a, \omega)$, where \mathbf{k}_a is the crossing point close to $(\pi/2, \pi/2)$. In fact, $\text{Im} \Sigma(\mathbf{k}_b, \omega)$ starts to develop an additional feature which eventually leads to the formation of a pseudogap in the spectra along the $M \rightarrow X$ direction at lower temperatures.²² In addition, one observes a rather large residual scattering rate for both momenta \vec{k}_a and \vec{k}_b . This can either be taken as further evidence for NFL behavior or as a signal for the occurrence of a new very small low-energy scale.³⁵ Obviously, we cannot decide on the answer to this question on the basis of the present data, but would have to look at much lower temperatures. Unfortunately, this is not possible at present. Note that in the low-energy regime the self-energy displays significant k dependence. This clearly renders theories based on a local approximation such as the DMFT inadequate at least for small doping.

At higher doping, Fig. 3, the peaks in the spectrum close to the Fermi energy are far sharper. Here it makes sense to speak of a conventional Fermi liquid and quasiparticles again. As already mentioned, the Fermi energy crossings can be found along $\Gamma \rightarrow M$ and $X \rightarrow \Gamma$. Again, this is in qualitative accordance with ARPES experiments for strongly overdoped Bi2212, Bi2201, and LSCO,^{3,36} although the experiments on LSCO still find rather broad structures even in heavily overdoped samples. In addition, there is no evidence for particle-hole asymmetry in our data. Especially at $(\pi/2, \pi/2)$ the structure crossing the Fermi level appears to be rather symmetric with respect to the crossing point.

The absolute value of the imaginary part of the self-energy, shown in Fig. 3(d), has a broad minimum at $\omega = 0$ with a very small residual scattering rate and changes little as \mathbf{k} moves along the Fermi surface. This weak dependence on \mathbf{k} is an indication that approximations such as the DMFT should be accurate here, i.e., that there is little effect of non-local correlations. All indications are that for this doping regime standard Fermi-liquid behavior has returned.

More evidence for NFL behavior can be seen in the shape of the Fermi surface. Theoretically, the Fermi surface can be defined in two different ways. First, the gradient of the electronic distribution function, $|\nabla n(\mathbf{k})|$, has a maximum at the Fermi surface. From a computational point of view this quantity is very convenient, because it does not require the calculation of dynamical properties. However, especially for a comparison with experimental Fermi-surface mappings based on ARPES experiments, the approach via $|\nabla n(\mathbf{k})|$ is probably not adequate, mainly due to the unknown influence of matrix elements in the experimental spectra.²

An analysis of the Fermi surface for the t - J model based on a study of $|\nabla n(\mathbf{k})|$ has been performed recently within a high-temperature expansion¹⁶ and been considered as clear

evidence for a violation of Luttinger's theorem and the possible formation of a non-Fermi liquid at small doping. Our results for that quantity are collected in Figs. 4 and 5, where $|\nabla n(\mathbf{k})|$ for the upper right quadrant of the first Brillouin zone (BZ) is shown in a density plot for $n = 0.95$ and $n = 0.8$, respectively. Regions of large values of $|\nabla n(\mathbf{k})|$ are colored in blue and violet, regions of small values in red. For comparison the Fermi surface for the noninteracting system is included (black lines). For small doping ($\delta = 0.05$), Fig. 4, $|\nabla n(\mathbf{k})|$ gives a rather broad structure around $(\pi/2, \pi/2)$ following the noninteracting Fermi surface. It is especially hard to define a Fermi surface at all or extract a reliable estimate of the Fermi surface volume from these results. As a consequence of the symmetry of $n(\mathbf{k})$ around $\mathbf{k} = (\pi, 0)$ and $(0, \pi)$, $|\nabla n(\mathbf{k})| = 0$ at these points, and as a result, $|\nabla n(\mathbf{k})|$ bifurcates around these points. This spurious symmetry-related effect is even observed for a cluster size $N_c = 1$ and thus is not driven by nonlocal correlations.

In accordance with the spectra in Fig. 3, the plot of $|\nabla n(\vec{k})|$ for large doping in Fig. 5 shows a fairly well-defined Fermi surface that coincides with the Fermi surface of the noninteracting system. Again, in contrast to the sharp peaks found in the spectra, $|\nabla n(\vec{k})|$ shows a substantial broadening, which in this case can, however, be explained by the conventional temperature broadening of Fermi's function.

An alternative way of mapping the Fermi surface is to make constant energy plots of the single-particle spectra at the Fermi energy $A(\mathbf{k}, \omega = 0)$. This method is equivalent to mapping out the regions in \mathbf{k} space where peaks in the spectral function $A(\mathbf{k}, \omega)$ cross the Fermi energy (see Figs. 2 and 3) and thus allows more direct contact with ARPES experiments. The constant energy plots $A(\mathbf{k}, \omega = 0)$ are shown in Figs. 6–8 for $n = 0.95$, $n = 0.90$, and $n = 0.80$, respectively, for the upper right quadrant of the first Brillouin zone. The regions of high density are colored in violet and low-density regions are in red. The solid black lines, as before, represent the noninteracting Fermi surface. To distinguish between structures resulting from either quasiparticle excitations or an incoherent background, we also plot the points where the real part of the denominator of the Green function vanishes at zero frequency. These points, which solve the quasiparticle equation $-\epsilon_{\mathbf{k}} - \text{Re} \Sigma(\mathbf{k}, \omega = 0) = 0$, are given by the solid red line.

For $n = 0.95$, the Fermi surface resulting from our calculations is holelike, centered around (π, π) , and encloses a volume larger than the noninteracting Fermi surface, indicating a violation of Luttinger's theorem. In addition, the shape of the Fermi surface close to $(\pi/2, \pi/2)$, especially the clear shift above $(\pi/2, \pi/2)$, cannot be interpreted neither in terms of a simple tight-binding band structure nor a weak-coupling theory.³² Note also that in comparison to the $|\nabla n(\mathbf{k})|$ result, no spurious bifurcation at $(\pi, 0)$ can be seen at this doping.

With increasing doping a bifurcation in the constant energy scan around $(\pi, 0)$ starts to develop (see Fig. 7), signaling the incipient crossover from a holelike Fermi surface to the expected electronlike surface at large doping. However,

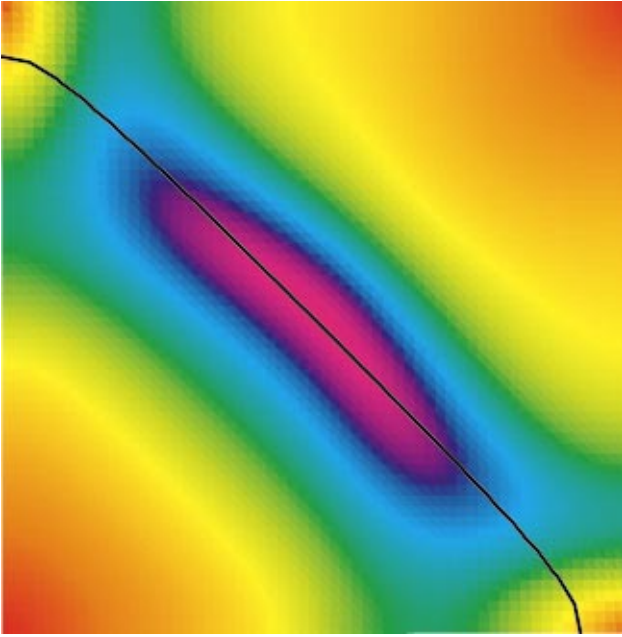


FIG. 4. (Color) Gradient of the distribution function $|\nabla n(\mathbf{k})|$ for $U=2$ eV, $T=\frac{1}{30}$ eV, $\delta=0.05$, and $N_c=16$. Shown is the upper right quadrant of the first BZ. The violet (red) represents regions of high (low) values. The blue and violet regions map out the Fermi surface. The noninteracting Fermi surface is shown by the black line. The interacting Fermi surface is rather hard to define. Note the strong bifurcation around the X points.

the points given by the red line that fulfill the quasiparticle equation do not show this bifurcation, indicating that the electronlike part in the constant energy scan closed around Γ

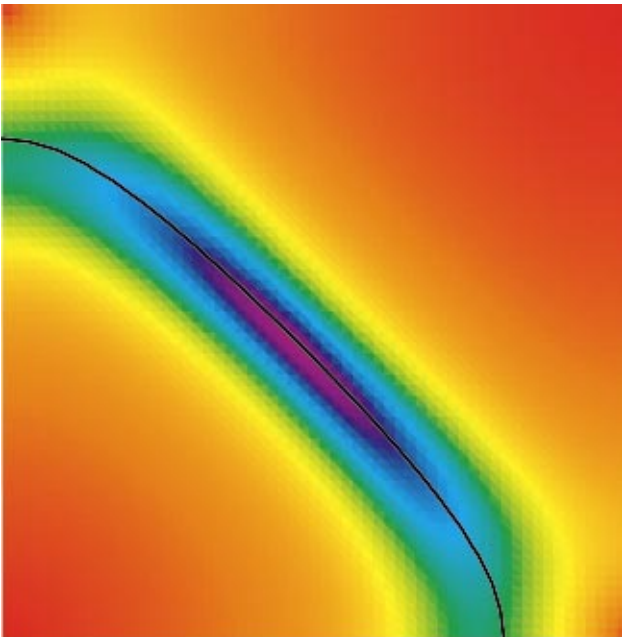


FIG. 5. (Color) $|\nabla n(\mathbf{k})|$ for $U=2$ eV, $T=\frac{1}{30}$ eV, $\delta=0.20$, and $N_c=16$. The color scheme is the same as in Fig. 4. The noninteracting and interacting Fermi surfaces coincide, in accord with Luttinger's theorem.

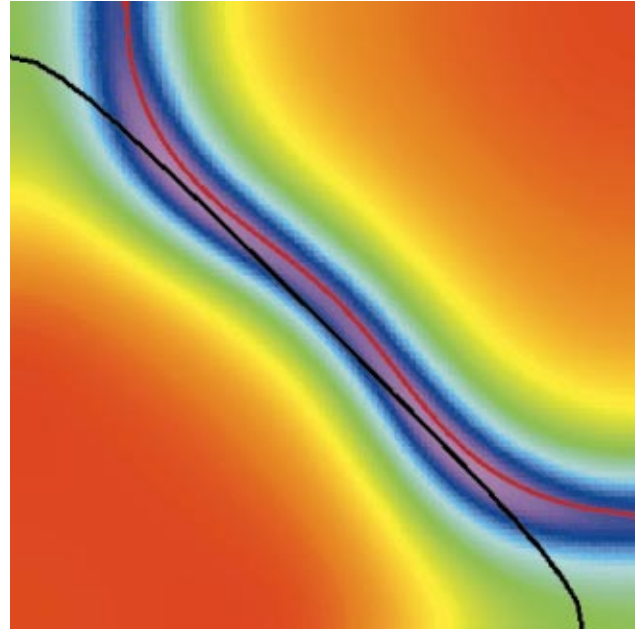


FIG. 6. (Color) Constant energy scans of $A(\mathbf{k}, \omega=0)$ for $U=2$ eV, $T=\frac{1}{30}$ eV, $\delta=0.05$, and $N_c=16$ in the right upper quadrant of the first BZ. The violet (red) represents regions of high (low) electronic density. The blue and violet regions map out the Fermi surface. The noninteracting Fermi surface is represented by a black line. The solid red line indicates the points where the real part of the denominator of the Green function vanishes. The interacting Fermi surface is holelike, centered at (π, π) , and encloses significantly more volume than the noninteracting Fermi surface. This indicates a violation of Luttinger's theorem.

is due to incoherent weight in the spectral function. In addition, around $(\pi/2, \pi/2)$ the peak in the spectrum follows more or less the noninteracting Fermi surface again. This points towards a restoration of Luttinger's theorem. For $n=0.80$, the Fermi surface is definitely electronlike, centered at $(0,0)$, and has essentially the same volume and shape as the noninteracting surface, indicating a return to Fermi-liquid-like behavior. No apparent remnants of the holelike Fermi surface and the incoherent structures seen at lower doping are left.

IV. SUMMARY AND CONCLUSIONS

The increasing precision and quality of experimental ARPES spectra in recent years have led to a number of additional results on the single-particle dynamics of the high- T_c cuprates, both partially resolving long-standing issues and posing new questions and problems. Motivated especially by the interesting observations concerning the changes of Fermi-surface topology with doping, we have studied the two-dimensional Hubbard model with nearest-neighbor hopping t in the intermediate coupling regime (on-site correlation U equal to the bandwidth) at the temperature $T=0.033$ eV. To study the model in this most problematic parameter regime we used a quantum Monte Carlo technique within the dynamical cluster approximation for the cluster size $N_c=16$. Since this method allows for controlled and

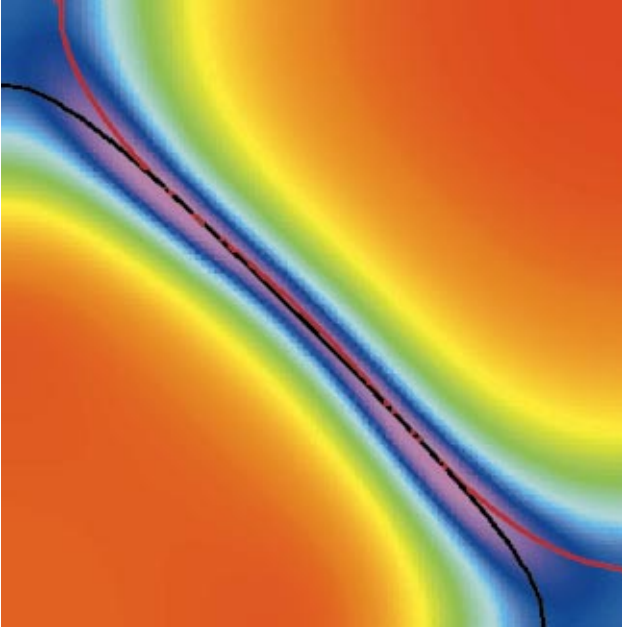


FIG. 7. (Color) Constant energy scans of $A(\mathbf{k}, \omega=0)$ for $\delta=0.1$. The other parameters and the color scheme are the same as in Fig. 6. The noninteracting and interacting Fermi surfaces start to coincide again, which can be interpreted as restoration of Luttinger's theorem. Note, however, the strong bifurcation around the X point with an electronlike part due to the incoherent background.

reliable calculations of low-energy features within a nonperturbative scheme and in the thermodynamic limit, fundamental problems in this field can be addressed. These include the single-particle spectral properties at low energies, especially possible deviations from Luttinger's theorem or the formation of non-Fermi-liquid states, and the resulting topology of the Fermi surface.

From the two different ways to define the Fermi surface, i.e., via $|\nabla n(\vec{k})|$ and inspection of a constant energy scan $A(\vec{k}, \omega=0)$, the latter turned out to be more precise. The constant energy scans are able to distinguish the situation in which a peak in the spectral function crosses the Fermi surface from where it only approaches it. Thus they were free of spurious symmetry-related bifurcations observed in the $|\nabla n(\vec{k})|$ plots. From the constant energy scans of the spectrum at the Fermi energy we find that the Fermi surface changes its topology compared to the noninteracting one as a function of decreased doping. While the latter is closed around the zone center for every finite doping, the interacting Fermi surface at low doping, $\delta=0.05$, is holelike, closed around $M=(\pi, \pi)$. Moreover, the form and shifts present in the Fermi surface must be taken as clear evidence of a violation of Luttinger's theorem. Non-Fermi-liquid behavior is also evidenced by the spectrum. A strong particle-hole asymmetry is found at the Fermi surface crossing near $(\pi/2, \pi/2)$ with holelike excitations having much longer lifetimes than electronic excitations. Furthermore the corresponding self-energy shows strong \vec{k} dependence rendering local approximations like the DMFT irrelevant. Additional structures in

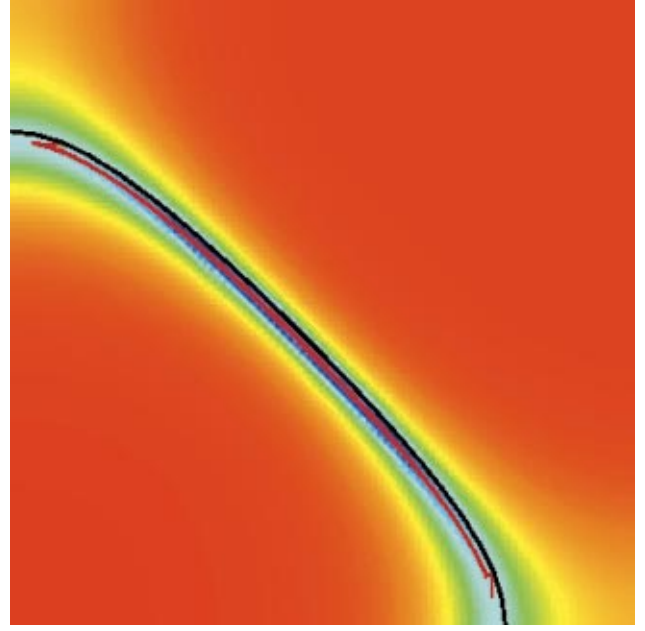


FIG. 8. (Color) Constant energy scans of $A(\mathbf{k}, \omega=0)$ for $\delta=0.2$. The other parameters and the color scheme are the same as in Fig. 6. The noninteracting and interacting Fermi surfaces coincide, in accord with Luttinger's theorem.

the self-energy and a rather large residual scattering rate can also be interpreted as signs for non-Fermi-liquid behavior. However, to really distinguish a non-Fermi liquid from a Fermi liquid with a possibly extremely small energy scale much lower temperatures must be studied.

With increased doping the Fermi surface changes its topology at $\delta \gtrsim 0.10$ to electronlike and from the topology around $(\pi/2, \pi/2)$ one can infer a tendency towards restoration of Luttinger's theorem and conventional Fermi liquid behavior. Finally when $\delta=0.20$ the Fermi surface is electronlike again, i.e., closed around the zone center, and coincides with the noninteracting Fermi surface. The corresponding spectra show well defined and sharp quasiparticle peaks around the Fermi energy with particle-hole symmetry being recovered in the low-energy region.

Although the Hubbard model surely presents an oversimplification of the real cuprates, the common belief is that at least the essential qualitative features of the low-energy dynamics should be reproduced. In particular, the results presented here show some interesting qualitative agreement with experiments regarding the behavior of the different structures observed in the spectra. Moreover, these features could be related to at least an apparent violation of Luttinger's theorem or possibly even non-Fermi-liquid behavior at low doping. From our results it becomes very clear that neither weak-coupling treatments nor local theories such as the DMFT are able to capture the essentials of the physics of the cuprate in the weakly doped regime. There are, of course, a variety of further questions to be addressed. For example, most of the interesting and controversial ARPES results are for Bi-based compounds, where a holelike Fermi surface is observed in the whole doping range in single and bilayer

systems. Thus, we conclude that the simple nearest-neighbor tight binding band structure used in this paper is definitely not sufficient to describe the cuprates and a detailed study of the influence of a finite and negative t' is necessary. Furthermore, the effects of bilayer coupling on the topology of the Fermi surface or more generally on the low-energy single-particle dynamics have to be investigated. We believe that such an investigation can also address some of the still mysterious features in the behavior of the Fermi-surface topology of the high- T_c cuprates. Moreover it is very important to find new methods to solve the DCA self-consistency cycle at lower temperatures or preferably at $T=0$. This would enable us to clearly distinguish between a strong-coupling Fermi liquid and genuine non-Fermi-liquid behavior at low doping.

ACKNOWLEDGMENTS

We acknowledge useful conversations with M. Hettler, C. Huscroft, H.R. Krishnamurthy, M. Sigrist, and T.M. Rice. This work was supported by the National Science Foundation (NSF) Grant No. DMR-0073308 and by the Deutsche Forschungsgemeinschaft through the Graduiertenkolleg “Komplexität in Festkörpern” and SFB Grant No. 484 “Kooperative Phänomene im Festkörper.” We acknowledge supercomputer support by the Leibniz Rechenzentrum in Munich under Grant No. h0301. This research was supported in part by the NSF Cooperative Agreement No. ACI-9619020 through computing resources provided by the National Partnership for Advanced Computational Infrastructure at the Pittsburgh Supercomputer Center.

- ¹For a review, see M.B. Maple, *J. Magn. Magn. Mater.* **177-181**, 18 (1998); J.L. Tallon and J.W. Loram, *Physica C* **349**, 53 (2001).
- ²S.V. Borisenko, A.A. Kordyuk, S. Legner, C. Dürr, M. Knupfer, M.S. Golden, J. Fink, K. Nenkov, D. Eckert, G. Yang, S. Abell, H. Berger, L. Forró, B. Liang, A. Maljuk, C.T. Lin, and B. Keimer, *Phys. Rev. B* **64**, 94513 (2001).
- ³A. Damascelli, D.H. Lu, and Z.-X. Shen, *J. Electron Spectrosc. Relat. Phenom.* **117-118**, 165 (2001).
- ⁴A. Kampf and J.R. Schrieffer, *Phys. Rev. B* **41**, 6399 (1990); *ibid.* **42**, 7967 (1990); P. Aebi, J. Osterwalder, P. Schwaller, L. Schlapbach, M. Shimoda, T. Mochiku, and K. Kadowaki, *Phys. Rev. Lett.* **72**, 2757 (1994).
- ⁵For an overview see, e.g., Ref. 3.
- ⁶A. Fujimori, A. Ino, T. Yoshida, T. Mizokawa, Z.-X. Shen, C. Kim, T. Kakeshita, H. Eisaki, S. Uchida, in *Open Problems in Strongly Correlated Electron Systems*, edited by J. Bonča, P. Prelovšek, A. Ramšak, and S. Sakar (Kluwer, Dordrecht, 2001), p. 119.
- ⁷T. Yoshida, X.J. Zhou, M. Nakamura, S.A. Kellar, P.V. Bogdanov, E.D. Lu, A. Lanzara, Z. Hussain, A. Ino, T. Mizokawa, A. Fujimori, H. Eisaki, C. Kim, Z.-X. Shen, T. Kakeshita, and S. Uchida, *Phys. Rev. B* **63**, 220501 (2001).
- ⁸A.A. Kordyuk, S.V. Borisenko, M.S. Golden, S. Legner, K.A. Nenkov, M. Knupfer, and J. Fink, cond-mat/0104294 (unpublished).
- ⁹P.V. Bogdanov, A. Lanzara, X.J. Zhou, S.A. Kellar, D.L. Feng, E.D. Lu, H. Eisaki, J.-I. Shimoyama, K. Kishio, Z. Hussain, and Z.X. Shen, cond-mat/0005394 (unpublished).
- ¹⁰T. Sato, T. Kamiyama, Y. Naitoh, T. Takahashi, I. Chong, T. Terashima, and M. Takano, *Phys. Rev. B* **63**, 132502 (2001).
- ¹¹Y.-D. Chuang, A.D. Gromko, D.S. Dessau, Y. Aiura, Y. Yamaguchi, K. Oka, A.J. Arko, J. Joyce, H. Eisaki, and S. I Uchida, K. Nakamura, and Yosichi Ando, *Phys. Rev. Lett.* **83**, 3717 (1999); D.L. Feng, W.J. Zheng, K.M. Shen, D.H. Lu, F. Ronning, J.-I. Shimoyama, K. Kishio, G. Gu, D. van der Marel, and F.X. Shen, cond-mat/9908056 (unpublished).
- ¹²Y.-D. Chuang, A.D. Gromko, A. Fedorov, Y. Aiura, K. Oka, Yoichi Ando, H. Eisaki, S.I. Uchida, and D.S. Dessau, *Phys. Rev. Lett.* **87**, 117002 (2001); Y.-D. Chuang, A.D. Gromko, A.V. Fedorov, Y. Aiura, K. Oka, Yoichi Ando, and D.S. Dessau, cond-mat/0107002 (unpublished).
- ¹³D.L. Feng, N.P. Armitage, D.H. Lu, A. Damascelli, J.P. Hu, P. Bogdanov, A. Lanzara, F. Ronning, K.M. Shen, H. Eisaki, C. Kim, and Z.-X. Shen, *Phys. Rev. Lett.* **86**, 5550 (2001); D.L. Feng, C. Kim, H. Eisaki, D.H. Lu, K.M. Shen, F. Ronning, N.P. Armitage, A. Damascelli, N. Kaneko, M. Greven, J.-i. Shimoyama, K. Kishio, R. Yoshizaki, G.D. Gu, Z.-X. Shen, cond-mat/0107073 (unpublished).
- ¹⁴P.W. Anderson, *The Theory of Superconductivity in the High- T_c Cuprates* (Princeton University Press, Princeton, NJ, 1997).
- ¹⁵E. Dagotto, *Rev. Mod. Phys.* **66**, 763 (1994).
- ¹⁶W.O. Putikka, M.U. Luchini, and R.R.P. Singh, *Phys. Rev. Lett.* **81**, 2966 (1998).
- ¹⁷N.E. Bickers, D.J. Scalapino, and S.R. White, *Phys. Rev. Lett.* **62**, 961 (1989).
- ¹⁸M.H. Hettler, A.N. Tahvildar-Zadeh, M. Jarrell, T. Pruschke, and H.R. Krishnamurthy, *Phys. Rev. B* **58**, 7475 (1998); M.H. Hettler, M. Mukherjee, M. Jarrell, and H.R. Krishnamurthy, *ibid.* **61**, 12 739 (2000).
- ¹⁹Th. Maier *et al.*, *Eur. Phys. J. B* **13**, 613 (2000); Th. Maier, M. Jarrell, Th. Pruschke, and J. Keller, *Phys. Rev. Lett.* **85**, 1524 (2000).
- ²⁰C. Huscroft, M. Jarrell, Th. Maier, S. Moukouri, and A.N. Tahvildarzadeh, *Phys. Rev. Lett.* **86**, 139 (2001).
- ²¹S. Moukouri and M. Jarrell, in *Computer Simulations in Condensed Matter Physics*, edited by D.P. Landau, K.K. Mon, and H.B. Schuttler (Springer-Verlag, Heidelberg, 2000), Vol. VII.
- ²²M. Jarrell, Th. Maier, C. Huscroft, and S. Moukouri, *Phys. Rev. B* **64**, 195139 (2001).
- ²³T. Pruschke, M. Jarrell, and J.K. Freericks, *Adv. Phys.* **42**, 187 (1995); A. Georges, and G. Kotliar, *Rev. Mod. Phys.* **68**, 13 (1996).
- ²⁴A.I. Lichtenstein and M.I. Katsnelson, *Phys. Rev. B* **62**, R9283 (2000).
- ²⁵G. Kotliar, S.Y. Savrasov, and G. Palsson, *Phys. Rev. Lett.* **87**, 186401 (2001).
- ²⁶Th. Maier and M. Jarrell, *Phys. Rev. B* **65**, 041104 (2002).
- ²⁷M. Jarrell, *Phys. Rev. Lett.* **69**, 168 (1992).

- ²⁸R. Bulla, Th. Pruschke, and A.C. Hewson, *J. Phys.: Condens. Matter* **10**, 8365 (1998).
- ²⁹J.E. Hirsch and R.M. Fye, *Phys. Rev. Lett.* **56**, 2521 (1986).
- ³⁰M. Jarrell and J.E. Gubernatis, *Phys. Rep.* **269**, 135 (1996).
- ³¹M.S. Hybertsen, E.B. Stechel, M. Schluter, and D.R. Jennison, *Phys. Rev. B* **41**, 11 068 (1990); S.B. Bacci, E.R. Gagliano, R.M. Martin, and J.F. Annett, *ibid.* **44**, 7504 (1991).
- ³²V. Zlatić, B. Horvatić, B. Dolički, S. Grabowski, P. Entel, and K.-D. Schotte, *Phys. Rev. B* **63**, 035104 (2001), and references therein.
- ³³C. Gros and R. Valenti, *Ann. Phys. (Leipzig)* **3**, 460 (1994).
- ³⁴S. Moukouri and M. Jarrell (unpublished).
- ³⁵J. Altmann, W. Brenig, and A.P. Kampf, *Eur. Phys. J. B* **18**, 429 (2000).
- ³⁶A. Ino, C. Kim, T. Mizokawa, Z.-X. Shen, A. Fujimori, M. Takaba, K. Tamasaku, H. Eisaki, and S. Uchida, *J. Phys. Soc. Jpn.* **68**, 1496 (1999).